Fitoterapia 134 (2019) 435–442

Contents lists available at ScienceDirect

Fitoterapia

journal homepage: www.elsevier.com/locate/fitote

New coumarins and monoterpene galloylglycoside from the stem bark of *Sapium baccatum*

Ting Li, Shanshan Wang, Peihong Fan*, Hongxiang Lou

Department of Natural Product Chemistry, Key Laboratory of Chemical Biology of Ministry of Education, School of Pharmaceutical Sciences, Shandong University, Jinan 250012, China

ARTICLE INFO

Keywords:
Sapium baccatum
Coumarins
Monoterpene galloylglycoside
Anti-inflammatory
Antifungal activity

ABSTRACT

Sapium baccatum has been traditionally used as therapeutic remedies. To support its medicinal benefits, our current phytochemical investigation attempted to further discover novel bioactive compounds from *S. baccatum*. Eight new phenolic compounds, namely, seven coumarins (**1–7**) and one monoterpene galloylglycoside (**8**), together with 23 (**9–31**) known compounds were isolated. Their structures were determined by extensive spectroscopic methods and comparison with literatures. The three pairs of enantiomers of **1**, **2** and **7** were confirmed on the basis of HPLC chiral analysis, electronic circular dichroism data and optical rotations. Two coumarins (**1–2**) were proven to be artifacts through HPLC analysis. The inhibitory effects on TNF-α secretion were examined biologically in LPS-induced BV2 microglia cells and all of the tested compounds exhibited significant inhibitory activity, especially new compound **1** possessed stronger inhibitory effects compared to the positive control quercetin. In addition, compounds **14** and **15** showed weak antifungal activity against *Candida albicans* SC5314 with MIC values both at 64 μg/mL. The results laid a solid foundation for additional research on *S.baccatum* related to its anti-inflammatory and antifungal medicinal value.

1. Introduction

Sapium baccatum (Euphorbiaceae) is a tall arboreal plant with edible sweet fruits that is distributed in China (Yunnan and Tibet) as well as most countries of south and southeast Asia, such as Vietnam, India, Malaysia, Sumatra, and Borneo (Kalimantan) [1–3]. This herb has been extensively used as ingredients in Chinese prescriptions for the treatment of scapulohumeral periarthritis, cerebral infarction, gouty arthritis, and other conditions. It has been also commonly used for treating abscess in Malaysia [4]. *S. baccatum* extracts have been proven to possess excellent antibacterial activity and toxic effects [5–7]. Previous phytochemical studies on the bark and leaves of *S. baccatum* have led to the isolation of various bioactive compounds, including eight triterpenoids, seven tannins, three aliphatic alcohol or derivatives, one alkaloid, and one flavonoid glycoside [2–12]. In continuing work to discover diverse compounds and biological effects, this study aimed to identify novel bioactive molecules from an ethanol extract of the stem bark of *S. baccatum*. Therefore, seven coumarins (**1–7**) and one monoterpene galloylglycosides (**8**) (Fig. 1) were isolated along with 23 known compounds (**9–31**). In addition, anti-inflammatory and antifungal activities of these compounds were evaluated.

2. Experimental section

2.1. General experimental procedures

Optical rotations were obtained on an MCP 200 (Anton Paar, Shanghai, China). UV spectra were detected by a UV-2450 spectrophotometer (Shimadzu, Kyoto, Japan). IR spectra were taken from KBr disk using a Nicolet Nexus 470 FT-IR spectrophotometer (Thermo Scientific, Waltham, MA, USA). HR-ESI-MS was implemented on a LTQ-Orbitrap XL (ThermoFinnigan, Bremen, Germany). ESI-MS data were obtained using an API 5500 Q-trap (AB SCIX, Concord, Ontario, Canada). ECD spectral analysis was performed on a Chirascan spectropolarimeter (Applied Photophysics, Leatherhead, UK). NMR spectra were measured on a Bruker Avance DRX-600 spectrometer (Bruker BioSpin Group, Billerica, MA, USA) at 600 (^{1}H) and 150 (^{13}C) MHz, using TMS as internal standard. CD_3OD and DMSO-d_6 were used as solvents (Sigma-Aldrich, Shanghai, China). HPLC was performed on an Agilent 1200 series system (Agilent Technologies) with an Eclispse XDB-C_{18} (250 mm × 4.6 mm, 5 μm; Agilent, Santa Clara, CA, USA). Semi-preparative HPLC separations were performed using a YMC-Pack ODS-A (250 mm × 10 mm, S–5 μm, 12 nm; YMC, Tokyo, Japan). HPLC chiral analysis was conducted on a Waters Delta 600 equipped with a

* Corresponding author.
E-mail address: fanpeihong@sdu.edu.cn (P. Fan).

https://doi.org/10.1016/j.fitote.2019.03.011
Received 6 February 2019; Received in revised form 16 March 2019; Accepted 16 March 2019
Available online 18 March 2019
0367-326X/

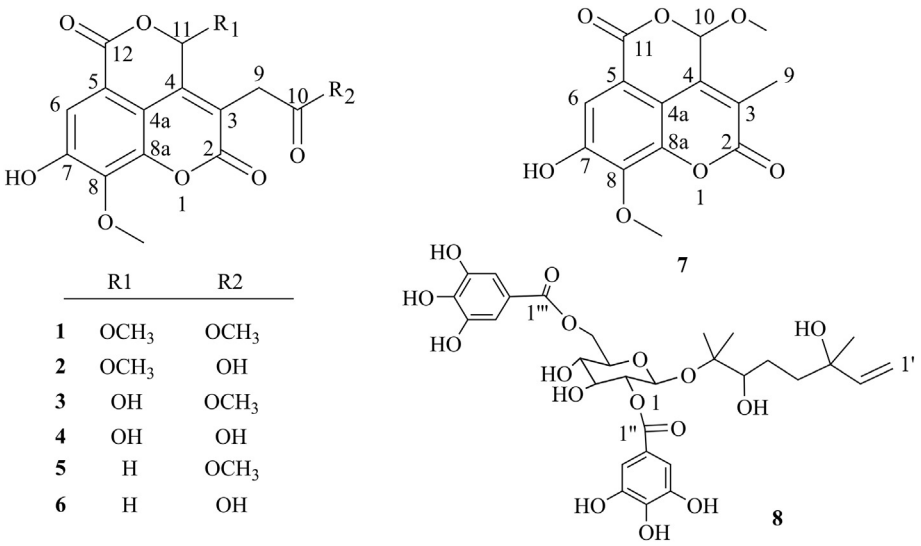

Fig. 1. The structures of the isolated compounds **1–8** from the stem bark of *S. baccatum*.

Waters 600 Controller and Waters 996 PDA detector (Waters, Milford, MA, USA) and a CHIRALPAK AD-H (250 mm × 4.6 mm, 5 μm; Daicel, Tokyo, Japan). High-speed countercurrent chromatography (HSCCC) was performed to isolate the compounds (TBE-30A, TBE−300B, Tauto Biotech, Shanghai, China). Medium-pressure liquid chromatography (MPLC) was used in purifying compounds on a DUAL Pump with EYELA UV 9000 detector (Servo Co., Ltd., Japan). Reversed phase C_{18} (ODS-A-HG, 12 nm, S-50 μm; YMC, Tokyo, Japan), silica gel (200–300 mesh; Qingdao Marine Chemical Inc., Qingdao, China), MCI gel (75–150 μm; Mitsubishi Chemical Corp., Tokyo Japan), toyopearl HW40 (45 μm; Tosoh Bioscience, Japan), Sephadex LH-20 (40–70 μm, Amersham Pharmacia Biotech AB, Uppsala, Sweden), and preparative TLC (HSGF 254, 0.4–0.5 mm; Yantai, China) were used in the course of isolation and purification.

2.2. Strains, cell culture, and chemicals

C. albicans SC5314 was obtained from School of Pharmaceutical Sciences, Shandong University (Jinan, China). BV2 microglia cells were obtained from the China Infrastructure of Cell Line Resources (Beijing, China). D-(+)-Glucose (Tokyo Chemical Industry Co., Ltd., Tokyo, Japan) was used as reference substance.

2.3. Plant material

The stem bark of *S. baccatum* was collected from Mengla County, Yunnan Province, PRC in November 2016 and identified by Chinese herbal medicine of Kunming Liezhi Sales Co., Ltd. A voucher specimen (20161118) was deposited in Dr. Fan's laboratory at the Department of Natural Products Chemistry, School of Pharmaceutical Sciences, Shandong University.

2.4. Extraction and isolation

The dried and powdered stem barks of *S. baccatum* (4.5 kg) were extracted thrice with 95% ethanol for 2 h at reflux. After evaporation of the filtrating solvents under reduced pressure, a part of the crude extract (500.0 g) was suspended in 90% CH_3OH (1 L) and fractionated with petroleum ether (1 × 3 L) to yield the PE extract (17.8 g). The evaporated CH_3OH residue was suspended in water (2 L) and then partitioned in EtOAC (2 × 5 L) to generate the EA extract (105.2 g) and H_2O extract (205.3 g). The PE extract (15.0 g) was subjected to column chromatography on silica gel and successively eluted with petroleum and EtOAC to yield eight fractions, designated as PEFr1–PEFr8. PEFr1 (4.0 g) was separated on a silica gel column repeatedly to yield compounds **20** (435.6 mg) and **30** (2.9 mg). PEFr2 (4.0 g) was also chromatographed using a similar procedure (silica gel) to yield five subfractions. Compounds **23** (138.8 mg) and **31** (6.0 mg) were obtained from the fourth subfractions by silica gel chromatography, and then compound **29** (10.5 mg) by Sephadex LH-20 and compound **26** (4.0 mg) by preparative TLC (petroleum ether-EtOAC 10:1). PEFr3 (3.5 g) was also separated into five subfractions (PEFr3.1–PEFr3.5) and constantly CC by silica gel chromatography to yield compounds **21** (6.0 mg) from PEFr3.1, **22** (20.0 mg) and **24** (209.8 mg) from PEFr3.4.

The EA extract (90.0 g) was fractionated into 13 subfractions (EAFr1–EAFr13) by silica gel chromatography. Compound **10** (21.3 mg) was precipitated as a yellowish solid in course of the isolation. Compound **9** (3.4 mg) was obtained from EAFr4 (140.1 mg) using toyopearl HW40 column and then reversed-phase HPLC (1.5 mL/min, 60%MeOH-0.01TFA, t_R = 20.0 min). EAFr5 (315.0 mg) was separated on a silica gel column and further purified by preparative TLC (petroleum ether-EtOAC 3.5:1) and preparative TLC (petroleum ether:acetone 5:1) to yield compound **25** (2.4 mg) and **28** (17.0 mg), respectively. EAFr9 (11.1 g) was subjected to a MCI chromatography and then a medium-pressure liquid chromatography (MPLC) eluted with gradient MeOH-H_2O to afford 17 fractions (EAFr9.1-EAFr9.17). EAFr9.2 was further separated into 14 fractions (EAFr9.2.1- EAFr9.2.14) using Sephadex LH-20. Further similar procedures on Sephadex LH-20, compound **12** (5.0 mg) and **13** (3.7 mg) were acquired from EAFr9.2.2. Compounds **1** (5.0 mg), **2** (4.0 mg), **3** (8.2 mg), and **27** (4.0 mg) were obtained from the EAFr9.2.5 by repetitive Sephadex LH-20 and preparative TLC (CH_2Cl_2-MeOH 9:1). EAFr9.3 was separated by CC on toyopearl HW40 eluting in a stepwise manner with MeOH-H_2O to yield 11 fractions (EAFr9.3.1-EAFr9.3.11). EAFr9.3.3 was chromatographed by Sephadex LH-20 using an isocratic elution of 50% MeOH-H_2O to obtain seven fractions (EAFr9.3.3.1-EAFr9.3.3.7). Compound **7** was obtained by RP-HPLC (47% MeOH-0.01% TFA, 1.5 mL/min, t_R = 23.0 min, 3.4 mg) from EAFr9.3.3.1. EAFr9.3.3.4 was purified on a silica gel and eluted with CH_2Cl_2-MeOH to yield compound **11** (8.1 mg) and EAFr9.3.3.7 through RP-HPLC with 38% MeOH (1.5 mL/min, t_R = 12.0 min) to provide compound **16** (12.3 mg). EAFr9.3.3.6 was separated by CC on MPLC and eluted with a gradient of MeOH-H_2O and then purified via RP-HPLC with 27% MeCN-0.01% TFA to yield compounds **4** (1.5 mL/min, t_R = 14.0 min, 10.5 mg) and **6** (1.5 mL/min, t_R = 16.0 min, 12.7 mg). EAFr9.7 was separated by Sephadex LH-20 continuously to yield compound **5** (3.0 mg). After using a similar process of separation on Sephadex LH-20, EAFr10 and EAFr12 were further purified by RP-HPLC to yield compounds **8** (60%MeOH, t_R = 13.0 min,

Table 1
^{1}H NMR spectral data of compounds **1–7**.

Position	1[a]	2[b]	3[b]	4[a]	5[a]	6[a]	7[a]
6	7.50, s	7.54, s	7.52, s	7.51, s	7.48, s	7.48, s	7.43, s
9	3.67, d (17.0)	3.69, d (17.0)	3.71, m	3.58, d (17.1)	3.58, s	3.49, s	2.08, s
	3.59, d (17.0)	3.58, d (16.9)		3.54, d (17.0)			
10							6.50, s
11	6.55, s	6.40, s	6.63, s	6.69, s	5.70, s	5.68, s	
8-OCH_3	3.94, s	4.08, s	4.06, s	3.96, s	3.96, s	3.95, s	3.94, s
10-OCH_3	3.62, s		3.71, m				3.59, s
11-OCH_3	3.53, s	3.66, s					
7-OH				11.09, s	11.08, s	11.05, s	
11-OH				8.57, s			
10-COOH				12.57, s			

[a] ^{1}H NMR data were measured in DMSO-d_6 at 600 MHz;
[b] ^{1}H NMR data were measured in CD_3OD at 600 MHz.

14.0 mg), **14** (22%MeCN, t_R = 14.0 min, 4.2 mg), **15** (22%MeCN, t_R = 22.0 min, 8.9 mg), and **17** (35% CH_3OH, t_R = 13.0 min, 10.8 mg).

Another part of the crude extract (500.0 g) was isolated by HSCCC (EtOAC-nBuOH-MeOH-H_2O 0.5: 2: 0.5: 4) to yield four fractions (Fr1–Fr4). Fr3 was purified by RP-HPLC to yield compounds **18** (55% MeOH-0.01%TFA, t_R = 23.5 min, 8.2 mg) and **19** (55% MeOH-0.01%TFA, t_R = 27.0 min, 3.7 mg).

2.4.1. Baccatune A (1)

Pale yellow, amorphous powder; [α]20 D-9.6 (c 0.10, MeOH); UV (MeOH) λ_{max} (log ε) 217 (3.00), 279 (2.48), 347 (2.60) nm; IR (KBr) ν_{max}: 3285, 2954, 2911, 2846, 1721, 1688, 1585, 1512, 1489 cm^{-1}; ^{1}H (600 MHz) and ^{13}C NMR (150 MHz) data (DMSO-d_6), see Tables 1 and 2; HR-ESI-MS: *m/z* 373.0532 $[M + Na]^+$ (Calcd. for $C_{16}H_{14}O_9Na$, 373.0530).

2.4.2. Baccatune B (2)

Pale yellow, amorphous powder; [α]20 D-11.2 (c 0.10, MeOH); UV (MeOH) λ_{max} (log ε) 220 (3.00), 281 (2.48), 347 (2.60) nm; IR (KBr) ν_{max}: 3340, 3232, 2959, 2924, 2854, 1711, 1600, 1509, 1484 cm^{-1} ; ^{1}H (600 MHz) and ^{13}C NMR (150 MHz) data (CD_3OD), see Tables 1 and 2; HR-ESI-MS: *m/z* 337.0556 $[M + H]^+$, (Calcd. for $C_{15}H_{13}O_8$, 337.0554).

2.4.3. Baccatune C (3)

Pale yellow, amorphous powder; [α]20 D-12.5 (c 0.10, MeOH); UV (MeOH) λ_{max} (log ε) 219 (3.18), 281 (3.01), 347 (3.50) nm; IR (KBr) ν_{max}: 3236, 2958, 1737, 1708, 1589, 1512 cm^{-1} ; ^{1}H (600 MHz) and ^{13}C NMR (150 MHz) data (CD_3OD), see Tables 1 and 2; ESI-MS: *m/z* 337.4 $[M + H]^+$.

Table 2
^{13}C NMR spectral data of compounds **1–7**.

Position	1[a]	2[b]	3[b]	4[a]	5[a]	6[a]	7[a]
2	160.4	162.3	162.7	160.4	159.8	159.9	160.8
3	117.0	120.2	116.7	117.6	112.6	113.6	119.8
4	139.2	140.6	143.4	141.0	142.1	141.6	137.0
4a	109.0,	111.6	110.7	109.6	110.6	110.7	109.1
5	115.1	116.2	116.2	115.1	115.7	115.6	113.8
6	114.4	115.4	116.0	113.7	113.7	113.4	114.2
7	156.0	155.4	156.9	153.7	154.0	153.8	154.9
8	139.5	140.8	140.9	138.9	138.7	138.7	139.4
8a	144.8	146.2	146.5	144.7	144.4	144.4	144.4
9	31.5	33.0	32.5	31.8	31.3	31.6	12.0
10	169.7	173.5	172.0	170.6	169.7	170.6	98.9
11	98.5	100.7	95.2	93.2	67.5	67.5	160.9
12	160.7	162.5	163.2	161.0	160.9	161.0	60.6
8-OCH_3	60.5	62.0	61.8	60.9	60.9	60.8	56.3
10-OCH_3	52.0		52.8		52.1		
11-OCH_3	56.0	57.1					

[a] ^{13}C NMR data were measured in DMSO-d_6 at 150 MHz;
[b] ^{13}C NMR data were measured in CD_3OD at 150 MHz.

2.4.4. Baccatune D (4)

White, amorphous powder; [α]20 D-10.5 (c 0.10, MeOH); UV (MeOH) λ_{max} (log ε) 219 (3.28), 281 (3.10), 346 (3.57) nm; IR (KBr) ν_{max}: 3298, 1688, 1583, 1511 cm^{-1} ; ^{1}H (600 MHz) and ^{13}C NMR (150 MHz) data (DMSO-d_6), see Tables 1 and 2; ESI-MS: *m/z* 321.3 $[M-H]^-$.

2.4.5. Baccatune E (5)

Pale yellow, amorphous powder; UV (MeOH) λ_{max} (log ε) 217 (3.78), 279 (3.35), 340 (3.50) nm; IR (KBr) ν_{max}: 3298, 2958, 2845,1691, 1583, 1510 cm^{-1} ; ^{1}H (600 MHz) and ^{13}C NMR (150 MHz) data (DMSO-d_6), see Tables 1 and 2; ESI-MS: *m/z* 319.3 $[M-H]^-$.

2.4.6. Baccatune F (6)

White, amorphous powder; UV (MeOH) λ_{max} (log ε) 218 (3.59), 281 (3.17), 347 (3.32) nm; IR (KBr) ν_{max}: 2938, 1707, 1649, 1586, 1514 cm^{-1} ; ^{1}H (600 MHz) and ^{13}C NMR (150 MHz) data (DMSO-d_6), see Tables 1 and 2; ESI-MS: *m/z* 305.4 $[M-H]^-$.

2.4.7. Baccatune G (7)

Pale yellow, amorphous powder; UV (MeOH) λ_{max} (log ε) 220 (3.74), 283 (3.62), 346 (4.00) nm; IR (KBr) ν_{max}: 3288, 2950, 2846, 1736, 1701, 1597, 1511, 1490, 1439, 1372 cm^{-1} ; ^{1}H (600 MHz) and ^{13}C NMR (150 MHz) data (DMSO-d_6), see Tables 1 and 2; ESI-MS: *m/z* 293.2 $[M + H]^+$.

2.4.8. 3,7-Dimethyl-1-octen-3,6,7-triol-7-O-β-D-2,6-digalloylglucopyranoside (8)

Brown yellow, amorphous powder; [α]20 D-24.6 (c 0.10, MeOH), UV (MeOH) λ_{max} (log ε) 218 (3.16), 276 (3.59) nm; IR (KBr) ν_{max}: 3271, 2974, 1693, 1611, 1534, 1448, 1319 cm^{-1}; ^{1}H (600 MHz) and ^{13}C NMR (150 MHz) data (CD_3OD and DMSO-d_6), see Table 3; HR-ESI-MS: *m/z* 659.1938 $[M-H_2O + Na]^+$, (Calcd for $C_{30}H_{36}O_{15}Na$, 659.1946).

2.5. Chiral analysis of compounds 1, 2 and 7

Briefly, compounds **1**, **2** and **7** were analyzed via HPLC under the following conditions: column, Chiralpak AD-H (250 × 4.6 mm, 5 μm); column temperature, 25 °C; flow rate: 1 mL/min; detector, Waters 996 PDA. Compound **1**: mobile phase: n-hexane:isopropanol (90/10, *v*/v) with 0.1% TFA; retention time, 28.24 and 31.15 min; Compound **2**: mobile phase: n-hexane/ethanol (90/10, v/v) with 0.1% TFA; retention time, 218.05 and 226.47 min; Compound **7**: mobile phase: n-hexane:isopropanol (90/10, v/v); retention time, 17. 19 and 20.25 min.

2.6. Acid hydrolysis of compound 8 and sugar analysis

Compound **8** (5 mg) was added to a mixture of 1.5 mL of concentrated HCl, 3 mL of H_2O, and 5 mL of dioxane and reacted under 100 °C for 2 h. H_2O was added to the reaction mixture and then extracted with CH_2Cl_2 (3 × 10 mL) after completion of the reaction. The aqueous layer was neutralized with Na_2CO_3 and concentrated under reduced pressure and then purified on Sephadex LH-20 (MeOH) column to obtain the sugar fraction. A solvent system (ethyl acetate:pyridine:ethanol:water 8:2:2:1) was used for TLC identification by comparison of R_f and optical rotation with an authentic sample: D-Glucose, R_f = 0.2 and optical rotation: [α]20 D + 45.0 (c 0.1, H_2O).

2.7. Bioactivity assays

Compounds (**1**, **5**, **6**, **8**, **12**, **13**, **14**, **15**, **18** and **22**) were tested for

Table 3
^{1}H NMR and ^{13}C NMR spectral data of compound **8**.

Position	**8**[a]		**8**[b]	
	δ_H	δ_C	δ_H	δ_C
1	4.88, m	97.0	4.78, d (8.1)	95.0
2	4.90, m	75.6	4.68, dd (9.4, 8.2)	73.8
3	3.68, m	76.4	3.51, t (9.1)	74.3
4	3.50, m	72.2	3.31, m	70.5
5	3.66, m	75.2	3.58, m	73.5
6	4.55, dd (11.7, 2.0)	65.0	4.45, dd (11.6, 1.6)	63.6
	4.41, dd (11.8, 6.5)		4.23, dd (11.8, 6.6)	
1′	5.11, dd (17.4, 1.5)	111.9	5.08, dd (17.4, 1.7)	111.1
	4.86 m		4.84, dd (10.8, 1.7)	
2′	5.88, dd (17.4, 10.8)	145.4	5.84, dd (17.4, 10.8)	144.8
3′		84.4		82.2
3′-CH_3	1.15, s	25.7	1.09, s	25.1
4′	1.54, m	38.4	1.48, m	37.0
	1.70, m		1.58, m	
5′	1.72, m	27.6	1.63, m	25.8
6′	3.75, t (6.7)	86.1	3.62, t (6.7)	83.7
7′		80.32		78.2
7′-CH_3	1.13, s	23.7	1.03, s	23.3
7′-CH_3	1.12, s	23.2	1.03, s	22.1
1″		121.4		119.4
2″	7.10, s	110.3	6.97, s	108.7
3″		146.5		145.4
4″		139.8		138.4
5″		146.5		145.4
6″	7.10, s	110.3	6.97, s	108.7
7″		167.5		164.8
1‴		121.7		120.0
2‴	7.11, s	110.2	6.96, s	108.6
3‴		146.4		144.5
4‴		139.7		138.1
5‴		146.4		144.5
6‴	7.11, s	110.2	6.96, s	108.6
7‴		168.3		165.7
3′-OH			5.4, s	
6′-OH			5.3, s	
Galloyl-OH			9.2, s	
			8.6, s	

[a] ^{1}H NMR data were measured in CD_3OD at 600 MHz, ^{13}C NMR at 150 MHz;
[b] ^{1}H NMR data were measured in DMSO-d_6 at 600 MHz, ^{13}C NMR at 150 MHz.

anti-inflammatory activity on LPS-induced BV2 microglia cells. The secretion of TNF-α in the culture supernatants of the LPS-induced BV2 microglia cells was assessed using the same method as described in the Ref [13], with minor modifications in that quercetin was used as positive control.

The MIC values of the compounds (**1**, **5**, **10**, **11**, **13**, **14**, **15**, **16**, **26**, **27**, and **28**) against *C. albicans* SC5314 were measured using the broth microdilution based on the Clinical and Laboratory Standards Institute (CLSI) guidelines (M27-A3), in accord with Ref [14].

3. Results and discussion

Traces of compounds **1–7** showed intense yellow fluorescence signals on TLC under UV 365 nm. During isolation and purification of these compounds, compounds **1** and **2** were observed to emerge from the methanol solution of pure compounds **3** and **4,** respectively. The methanol solutions of **3** and **4** that were deposited at room temperature were measured using HPLC analysis at three time intervals (0, 4, and 10 days) [15]. The results showed that compounds **1** and **2** were artifacts due to the occurrence of additional new peaks that emerged in a time-dependent manner (Fig. 2).

Compound **1** was obtained as a pale yellow solid, with a molecular formula of $C_{16}H_{14}O_9$ as determined by HR-ESI-MS at *m/z* 373.0532 ($[M + Na]^+$, $C_{16}H_{14}O_9Na$ calcd. 373.0530), indicating 10 degrees of unsaturation. The IR spectra displayed absorption bands at 3285 cm^{-1} (hydroxyl), 2954 cm^{-1} (methyl), 2911, 2846 cm^{-1} (methylene), 1721, 1688 cm^{-1} (carbonyl groups), 1585, 1512, and 1489 cm^{-1} (phenyl group). ^{1}H NMR (Table 1) revealed three methoxy groups at δ_H 3.94 (3H, s, 8-OCH_3), 3.62 (3H, s, 10-OCH_3), and 3.53 (3H, s, 11-OCH_3) and a methylene group at δ_H 3.67 (1H, d, J = 17.0 Hz, H-9a) and 3.59 (1H, d, J = 17.0 Hz, H-9b). The combined elucidation of the ^{13}C NMR (Table 2) and HSQC data suggested 16 carbon signals that were attributed to three oxygenated methyls (δ_C 52.0, 56.0, 60.5; C-10, C-11, 8-OCH_3 respectively), one sp^3 methylene (δ_C 31.5, C-9), one sp^3 methine (δ_C 98.5, C-11), one sp^2 methine (δ_C 114.4, C-6), seven sp^2 quaternary carbons (δ_C 117.0, 139.2, 109.0, 115.1, 156.0, 139.5, 144.8; C-3, C-4, C-4a, C-5, C-7, C-8, C-8a, respectively), and three carbonyl groups (δ_C 160.4, 169.7, 160.7 ; C-2, C-10, C-12, respectively). Nine carbons, namely, C-2 (δ_C 160.4), C-3 (δ_C 117.0), C-4 (δ_C 139.2), C-4a (δ_C 109.0), C-5 (δ_C 115.1), C-6 (δ_C 114.4), C-7 (δ_C 156.0), C-8 (δ_C 139.5), and C-8a (δ_C144. 8) could be attributed to a coumarin skeleton. The HMBC correlations (Fig. 3) from H-6 (δ_H 7.50) to C-4a, C-5, C-7, and C-8 verified the coumarin skeleton. The methine proton at δ_H 6.55 (1H, s, H-11) was located at position C-11 (δ_C 98.5) based on HSQC correlation. Based on the HMBC correlation of the methine proton H-11 (δ_H 6.55) to C-3, C-4, C-4a, and C-12, the lactonic ring unit was confirmed to be substituted at C-4 and C-5. The HMBC correlation from H-9a and H-9b to C-2, C-3, C-4, and C-10 suggested the position of a carboxymethyl group at C-3. The locations of three methoxy groups were determined by HMBC correlations of δ_H 3.94, 3.62, 3.53 with C-8, C-10, and C-11, respectively. A literature search revealed that the chemical structure of **1** is similar to phyllanthusiin E from the leaves of *Phyllanthus flexuosus*, except for the presence of three methoxy groups [16]. Thus, the planar structure of **1** was established. To elucidate the configuration of the only one chiral center at C-11, chiral analysis was performed by HPLC, and a pair of peaks with the area ration of approximately 1:1 was observed. **1a** and **1b** were obtained through HPLC semipreparation, and their ECD spectra were measured as obvious positive and negative Cotton effect at 220 nm (Fig. 4). The configuration of **1a** and **1b** were proposed to be *S* and *R* configuration respectively on the basis of optical rotations **1a**: [α]20D + 24.4 (c 0.05, MeOH) and **1b**: [α]20 D-26.0 (c 0.05, MeOH), in comparison with *S* configuration of dehydropicrorhiza acid methyl diester ([α]14D + 17.7 (c 0.2, MeOH), which have similar structure pattern [17]. Thus, **1** existed as a pair of enantiomers (*S* and *R* configuration, Fig. 4). As **1** possesses a basic skeleton similar to **2–7**, for convenience, we have assigned the trivial name Baccatune A.

Compound **2** was obtained as a pale yellow solid, whose molecular formula was confirmed to be $C_{15}H_{12}O_9$ determined by HR-ESI-MS at *m/z* 337.0556 ($[M + H]^+$, $C_{15}H_{13}O_9$ calcd. 337.0554), indicating 10 degrees of unsaturation. The IR spectrum revealed the existence of 3232 cm^{-1} (hydroxyl), 2959 cm^{-1} (methyl), 2924, 2854 cm^{-1} (methylene), 1711 cm^{-1} (carbonyl group), 1600, 1509, and 1484 cm^{-1} (phenyl group), in addition to the absorption bands at 3340 cm^{-1} (carboxyl group). Comparison of NMR data with **1** suggested a structure with the same coumarin skeleton. However, the number of methoxy groups differed from **1** based on the presence of a terminal carboxylic acid moiety and the absence of correlated protons signal of 10-OCH_3 to C-10 (δ_C 173.5) in HMBC correlations. The remaining correlations in the 2D spectra were comparable to **1**. Chiral analysis of **2** indicated a pair of peaks with an area of approximately 1:1, indicating that **2** is a pair of enantiomers. Therefore, the structure of **2** was determined as Baccatune B.

Compound **3** was obtained as a pale yellow solid, and its molecular formula was determined at *m/z* 337.4 by positive ESI-MS, which together with ^{13}C NMR spectroscopy (15 carbons) suggested a molecular formula of $C_{15}H_{12}O_9$. The IR spectrum indicated the presence of peaks at 3236 cm^{-1} (hydroxyl), 2958 cm^{-1} (methyl), 1737, 1708 cm^{-1} (carbonyl groups), 1589 and 1512 cm^{-1} (phenyl group). Compared to **1**, a methoxy carbon (11-OCH_3) was not present in the ^{13}C NMR spectrum of **3**. This can be verified by absence of CH_2 with 14 *m/z* units

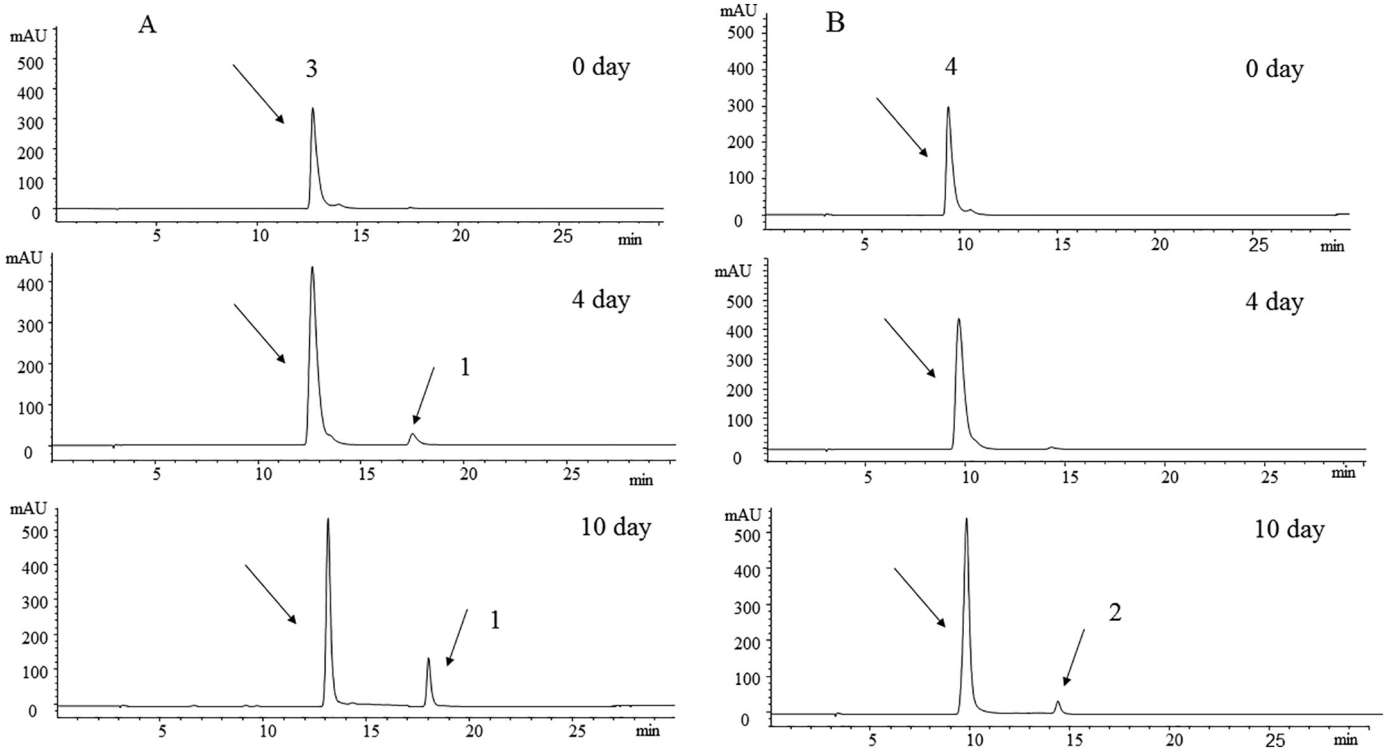

Fig. 2. Time-dependent emergence of artifacts **1–2** in a methanol solution of **3–4.** (A) the emergence of **1** from **3**; (B) the emergence of **2** from **4**.

when compared to **1**. HMBC correlations in the methine proton δ_H 6.63 (1H, s, H-11) still occurred at C-3 (δ_C 116.7), C-4a (δ_C 110.7), and C-12 (δ_C 163.2), indicating a hydroxy group substituted at C-11. A methylene was located via HMBC correlations of its protons at δ_H 3.71 (overlapping) with C-2 (δ_C 162.7), C-3 (δ_C 116.7), C-4 (δ_C 143.4), and C-10 (δ_C 172.0). The observed 1D and 2D NMR of the remaining part of the molecule are similar to **1**. Therefore, the structure of **3** was determined to be Baccatune C. The chiral center at C-11 of **3** may exist as *S* and *R* configuration based on their similar ECD spectrum and optical rotation to **1** and **2**.

Compound **4** was obtained as a white solid, and its molecular formula was measured at *m/z* 321.3 ([M-H]$^-$) based on the negative ESI-MS, which together with ^{13}C NMR spectroscopy (14 carbons) suggested a molecular formula of $C_{14}H_{10}O_9$. The IR spectrum indicated the presence of peaks at 3298 cm^{-1} (hydroxyl), 1688 cm^{-1} (carbonyl groups), 1583, and 1511 cm^{-1} (phenyl group). Furthermore, the ^{1}H NMR and HSQC data of **4** exhibited three hydroxy group signals at δ_H 11.09 (1H, s, 7-OH), δ_H 8.57 (1H, s, 11-OH), and δ_H 12.57 (1H, s, 10-COOH), suggesting that C-10 (δ_C 170.6) and C-11 (δ_C 93.2) were substituted by OH instead of OCH_3, which is in contrast to **1**. This was also confirmed by the ESI-MS difference of the 48 *m/z* unit. Except for the HMBC correlation at δ_H 6.69 (1H, s, H-11) to C-3 (δ_C 117.6), C-4a (δ_C 109.6), and C-12 (161.0), HMBC correlations of H-6 and H-9 were coincided with **1**. Thus, compound **4** was assigned as Baccatune D.Compound **4** may be mixtures of a pair of enantiomers as well owning to its similar ECD spectrum and optical rotation to **1** and **2**.

Compound **5** was obtained as a pale yellow solid, and its molecular formula was determined at *m/z* 319.3 ([M-H]$^-$) based on the negative ESI-MS, which together with ^{13}C NMR spectroscopy (15 carbons), suggested a molecular formula of $C_{15}H_{12}O_8$, corresponding to one oxygen less than **3**. The IR spectrum indicated the presence of peaks at 3298 cm^{-1} (hydroxyl), 2958, 2845 cm^{-1} (methyl), 1691 cm^{-1} (carbonyl groups), 1583, and 1510 cm^{-1} (phenyl group). The HSQC spectrum revealed that a methylene at δ_H 5.70 (2H, s, H-11) and δ_C 67.5 (C-11) of **5** differed from that of **3** at δ_H 6.63 (1H, s, H-11) and δ_C 95.2 (C-11). An 27.7 ppm upfield shift of C-11 indicated the absence of hydroxy group at C-11, which was supported by the mass difference of the 16 *m/z* unit in contrast to **3**. HMBC correlations of the 7-OH proton (δ_H 11.08) to C-8 (δ_C 138.7), C-7 (δ_C 154.0), C-6 (δ_C 113.7) and 8-OCH_3 (δ_H 3.96) to C-8 (δ_C 138.7) indicated that substituents of OH and OCH_3 were assigned at adjacent carbons at C-7 (δ_C 154.0) and C-8 (δ_C 138.7), respectively. The 1D NMR data of **5** was similar to that of phyllanthusiin E methyl ester, in which a hydroxy group rather than a methoxy group was substituted at C-8 [18]. Thus, compound **5** was assigned as Baccatune E.

Similarly, the NMR spectra of **6** indicated a similar coumarin skeleton as **5**, with the presence of two methylene protons at δ_H 5.68 (2H, s, H-11) and 3.49 (2H, s, H-9), an aromatic proton at δ_H 7.48 (1H, s, H-6), and one oxygenated methyl signal at δ_H 3.95 (3H, s, 8-OCH_3). However, no methyl ester was substituted on C-10 compared to **5,** and the mass spectrometric data of decreasing CH_2 units were in complete agreement with the measured molecular constitution of **6** (*m/z* 305.2 [M-H]$^-$). Thus, compound **6** was assigned as Baccatune F.

Compound **7** was obtained as a pale yellow solid, and its molecular formula was determined at *m/z* 293.2 ([M + H]$^+$) based on the positive ESI-MS. The IR spectrum indicated the presence of peaks at 3288 cm^{-1} (hydroxyl), 2950, 2846, 1439, 1372 cm^{-1} (methyl), 1736, 1701 cm^{-1} (carbonyl groups), 1597, 1511 and 1490 cm^{-1} (phenyl group). A detailed analysis of its ^{1}H NMR spectrum exhibited the presence of three methyls signals at δ_H 3.94 (3H, s, 8-OCH_3), 3.59 (3H, s, 10-OCH_3), and 2.08 (3H, s, H-9); one oxygenated methine proton at δ_H 4.65 (1H, s, H-10); and an aromatic proton at δ_H 7.43 (1H, s, H-6). Similarly, the 1D spectra established the presence of a coumarin skeleton, as shown in Tables 1 and 2. The HMBC correlations of **7** were comparable to **1**, expect HMBC correlations from H-9 (δ_H 2.08) to C-2 (δ_C 160.8), C-3 (δ_C 119.8), and C-4 (δ_C 137.0), which suggested that a methyl group was connected at C-3. Thus, the planar structure of **7** was established. The absolute configuration at C-10 of **7** was also elucidated by HPLC chiral analysis and optical rotations. **7a** and **7b** were obtained through HPLC semipreparation and their configurations were

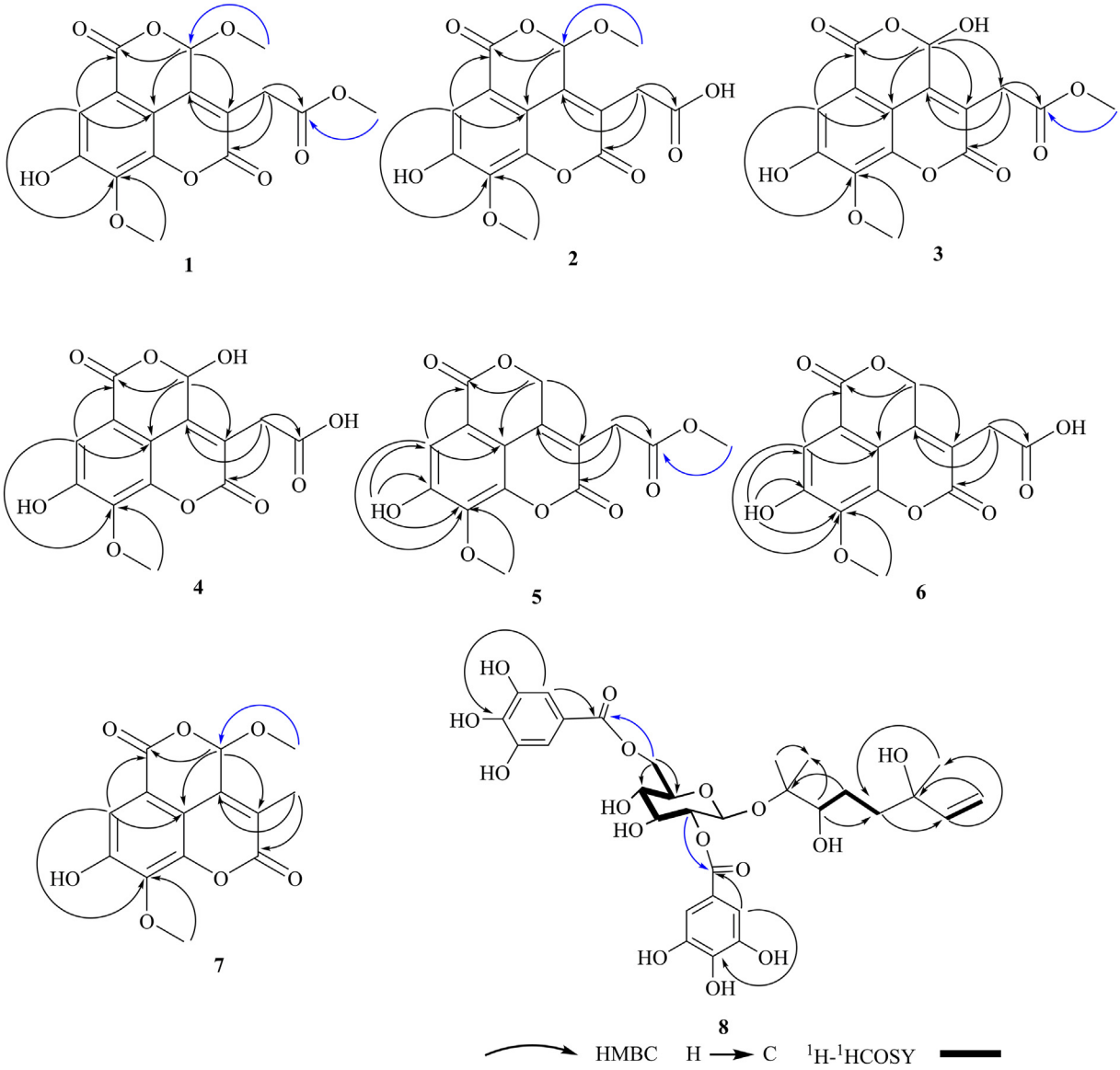

Fig. 3. Key HMBC and H—H COSY correlations of **1–8**.

confirmed be *S* and *R* configuration respectively on the basis of optical rotations **7a**: [*α*]20 D + 28.0 (c 0.05, MeOH) and **7b**:

[*α*]20 D-30.0 (c 0.05, MeOH). Thus, compound **7** existed as a pair of enantiomers and was assigned as Baccatune G.

Compound **8** was obtained as a brown solid. HR-ESI-MS of **8** afforded a $[M\text{-}H_2O + Na]^+$ peak at *m/z* 659.1938 ($C_{30}H_{36}O_{15}Na$ calcd. 659.1946), suggesting a molecular formula $C_{30}H_{38}O_{16}$ for **8**. The IR absorptions revealed the presence of peaks at 3271 cm^{-1} (hydroxy groups), 2974 cm^{-1} (methyls), 1693 cm^{-1} (ester carbonyls), and 1611 and 1534 cm^{-1} (phenyl groups). The presence of two galloyl moieties in **8** was proven by proton signals at δ_H 7.10 (2H, s, H-2″, H-6″), δ_H 7.11 (2H, s, H-2‴ and H-6‴) and the corresponding carbon signals at δ_C 168.3, 167.5, 146.5 (×2), 146.4 (×2), 139.8, 139.7, 121.7, 121.4, 110.3 (×2), and 110.2 (×2). The 1D NMR spectra also revealed the presence of one β-glucopyranosyl unit with its anomeric proton at δ_H 4.78 in DMSO-d_6 (1H, d, *J* = 8.1 Hz, H-1, overlapped by H_2O signal in CD_3OD). D-glucopyranosyl was confirmed based on TLC analysis of products obtained from acid hydrolysis followed by Sephadex LH-20 separation and optical rotation measurement [19,20]. The long-range HMBC correlations of δ_H 4.90 (overlapping, H-2) with C-1″ and those of δ_H 4.55 (1H, dd, *J* = 11.7, 2.0 Hz, H-6a), δ_H 4.41 (1H, dd, *J* = 11.8, 6.5 Hz, H-6b) with C-1‴ suggested the presence of a 2,6-digalloylglucopyranosyl moiety. In the remaining proton signals, ABX spin system signals at δ_H 5.88 (1H, dd, *J* = 17.4, 10.8 Hz), δ_H 5.11 (1H, dd, *J* = 17.4, 1.5 Hz), δ_H 4.86 (overlapping) were observed, which corresponded to a terminal vinyl group (δ_C 145.4, C-2′), (δ_C 111.9, C-1′). Proton signals at δ_H 1.15 (3H, s, 3′-Me), δ_H 1.13 (3H, s, 7′-Me), and δ_H 1.12 (3H, s, 7′-Me), together with carbon signals at δ_C 25.7(3′-Me), 23.7, and 23.2 (two 7′-Me) suggested the presence of three methyl groups. The terminal vinyl group and three methyl groups, together with the remaining five carbon signals (two quaternary carbons, two methylene carbons, and one oxygenated methine carbon), were confirmed to be a monoterpenoid moiety that is closely similar to 6,7-dihydroxy-6,7-dihydrolinalool [21]. The position of the glycosidic linkage was determined using NOESY spectroscopy. A NOE correlation was observed at δ_H 1.13, 1.12 (3H, each, s, 7′-Me,) with δ_H 4.88 (1H, overlapping, H-1), establishing the attachment of monoterpenoid aglycone on anomeric carbon. Consequently, the structure of compound **8** was assigned as 3,7-dimethyl-1-octen-3,6,7-triol-7-O-β-D-2,6-di-galloylglucopyranoside.

Known compounds were identified by comparison with the experimental and reported spectroscopic data: ellagic acid (**9**) [22], 3,3-di-*O*-

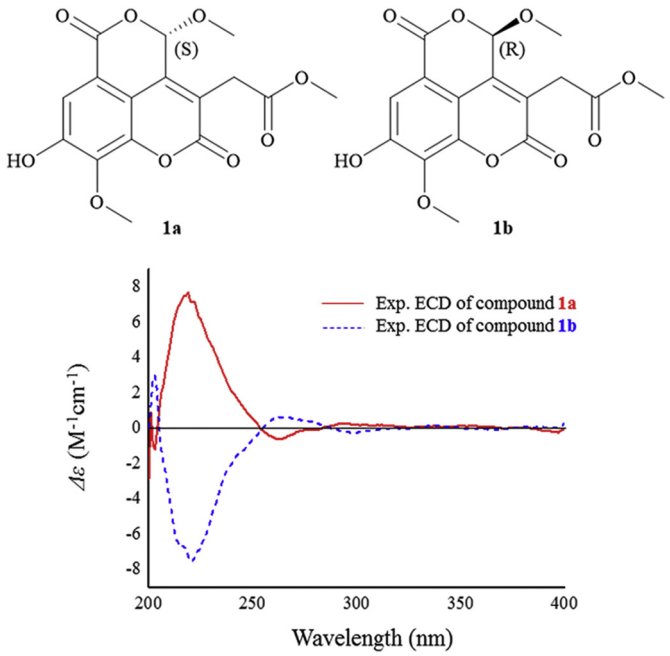

Fig. 4. ECD spectra and absolute configurations of compounds **1a** and **1b**.

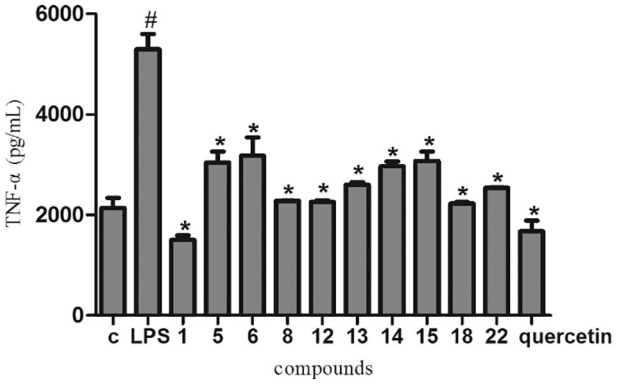

Fig. 5. Inhibitory effects on TNF-α secretion of the isolated compounds in LPS-induced inflammatory response with quercetin as positive control. BV2 microglia cells were pretreated with compounds (3 μg/mL) for 1 h and then stimulated with LPS at 100 ng/mL for 24 h. The supernatants were harvested and the secretion of TNF-α were measured by ELISA. The data are presented as mean ± SD from at least 3 independent experiments. *$p < 0.001$ as compared to the cells treated with LPS; #$p < 0.001$, as compared to the control.

methylellagic acid (**10**) [23], ethyl gallate (**11**) [24], brevifolin (**12**) [22], ethyl brevifolin carboxylate (**13**) [22], tercatain (**14**) [6], 1,2,3,4,6-penta-O-gally-β-D-glucopyranose (**15**) [24], isocorilagin (**16**) [25], coriagin (**17**) [22], 3,3′-di-*O*-methylellagicacid-4′-O-α-L-rhamnopyranoside (**18**) [26], 3,3′-di-*O*-methylellagicacid-4′-O-β-D-xylopyranoside (**19**) [27], taraxerone (**20**) [4], taraxerol (**21**) [4], 28-hydroxy-14-taraxeren-3-one (**22**) [28], 3-*O*-acetylaleuritolic acid (**23**) [8], β-sitosterol (**24**) [4], β-sitostenone (**25**) [29], chrysophanol (**26**) [30], scopoletin (**27**) [31], docosyl trans-isoferulate (**28**) [4], hexadecanoic acid (**29**) [32], squalene (**30**) [33], dibutyl phthalate (**31**) [34]. Among them, **9**, **11**, **12**, **13**, **15**, **16**, **18**, **19**, **22**, **25**, **26**, **27**, **29**, **30**, and **31** were isolated for the first time from *S. baccatum*.

Biological activity experiments showed that all of the tested compounds exhibited significantly comparable anti-inflammatory activity.

to the positive control quercetin in LPS-induced BV2 microglia cells. Compound **1** showed stronger inhibitory effects compared to the positive control quercetin (TNF-α 1503.51 pg/mL, 1674.44 pg/mL respectively) (Fig. 5).

An antifungal investigation demonstrated that the MIC values of **14** and **15** against *C. albicans* SC5314 were both 64 μg/mL, indicating weak antifungal activity. No obvious antifungal effects (MIC > 128 μg/mL) were observed in the other tested compounds in comparsion with Ref [14].

In summary, eight new compounds, including Baccatune A − G (**1–7**), 3,7-dimethyl-1-octen-3,6,7-triol-7-O-β-D-2,6-digalloylglucopyranoside (**8**) and 23 known compounds (**9–31**), were isolated from the stem bark of *S. baccatum*. Compounds **1** and **2** were confirmed as artifacts and assigned as two pairs of enantiomers via HPLC chiral analysis, ECD experiments and optical rotations. Compounds **3** and **4** may be mixtures of enantiomers as well owning to their similar ECD spectra and optical rotations to **1** and **2**, however, they were not successfully separated in present attempt. Compound **7** was confirmed as a pair of enantiomers via HPLC chiral analysis and optical rotations.

The bioassay results of the inhibitory effects of the tested compounds on LPS-induced TNF-α production revealed significant anti-inflammatory activity, explaining traditional use of *S. baccatum* from the other aspect in comparison with Ref [35]. The observed weak antifungal activity of the isolated tannins against *C. albicans* also justified the pharmacological effects of *S. baccatum* [6]. Based on traditional medicinal values of *S. baccatum*, additional studies to identify novel bioactive compounds are warranted.

Conflict of interest

The authors declare no competing financial interest.

Acknowledgments

This work was supported by the National Natural Science Foundation of China (Grant No. 81473323). Authors thank Dr. Chang of the same Lab for the performance of antifungal tests.

References

[1] H. Luo, J.J. Wu, X.L. Zhu, Z. Dan, Y.H. Tan, W. Hou, New records of three plants in Tibet, Acta Bot. Boreal. Occident. Sin. 36 (2016) 194–196, https://doi.org/10.7606/j.issn.1000-4025.2016.01.0194.
[2] Y. Ahmed, M.H. Sohrab, S.M. Al-Reza, F.S. Tareq, C.M. Hasan, M.A. Sattar, Antimicrobial and cytotoxic constituents from leaves of *Sapium baccatum*, Food Chem. Toxicol. 48 (2010) 549–552, https://doi.org/10.1016/j.fct.2009.11.030.
[3] H.J. Esser, A partial revision of the Hippomaneae (Euphorbiaceae) in Malesia, Blumea. 44 (1999) 149–215.
[4] L.M.R. Al Muqarrabun, N. Ahmat, S.R.S. Aris, N. Norizan, Phytochemical investigation of the stem bark of *Sapium baccatum (Roxb.)*, Aust. J. Basic Appl. Sci. 8 (2014) 432–438.
[5] Y.J. Ding, G.Y. Zuo, X.Y. Hao, G.C. Wang, J. Han, Screening of antibacterial activity of 20 Chinese herbal medicines in Yunnan, Afr. J. Pharm. Pharmacol 7 (2013) 2859–2860, https://doi.org/10.5897/AJPP2012.1513.
[6] T.T. Vu, H. Kim, V.K. Tran, H.D. Vu, T.X. Hoang, J.W. Han, Y.H. Choi, K.S. Jang, G.J. Choi, J.C. Kim, Antibacterial activity of tannins isolated from *Sapium baccatum* extract and use for control of tomato bacterial wilt, PLoS One 12 (2017) e0181499, , https://doi.org/10.1371/journal.pone.0181499.
[7] M. Taher, N.A.M. Alewi, S. Deny, Z. Zamli, N. Ramli, N. Saad, Toxic effects of *Sapium baccatum (Ludai)* extract in rats, Sains Malays. 41 (2012) 1423–1429.
[8] T.K. Ray, D.R. Misra, H.N. Khastgir, Phytosterols in euphorbiaceae and rutaceae, Phytochemistry 14 (1975) 1876–1877, https://doi.org/10.1016/0031-9422(75)85320-9.
[9] B. Saha, D.B. Paekar, D.R. Misra, B.P. Pradhan, H.N. Khaatgir, Baccatin, a novel nortriterpene peroxide isolated from *sapium baccatum roxb*, Tetrahedron Lett. 35 (1977) 3095–3098, https://doi.org/10.1016/S0040-4039(01)83168-3.
[10] D. Arbain, L.T. Byrne, J.R. Cannon, V.A. Patrick, A.H. White, (-)-Bukittinggine, the major alkaloid of *Sapium baccatum*: crystal structure and absolute configuration of bukittinggine hydrobromide, Aust. J. Chem. 43 (1990) 2795–2798, https://doi.org/10.1071/ch9900185.
[11] L.M.R. Al Muqarrabun, N. Ahmat, S.R.S. Aris, Chemical constituents of two Malaysian medicinal plants: *Scaphium Macropodum* (Sterculiaceae) and *Sapium Baccatum* (Euphorbiaceae), Proc. ICNP 4 (2013) 212.
[12] L.M.R. Al Muqarrabun, N. Ahmat, S.R. Aris, N. Norizan, N. Shamsulrijal, F.Z. Yusof, M.N. Suratman, M.I. Yusof, F. Salim, A new triterpenoid from *Sapium baccatum* (Euphorbiaceae), Nat. Prod. Res. 28 (2014) 1003–1009, https://doi.org/10.1080/14786419.2014.903396.
[13] Y.F. Zhou, S.S. Wang, H.X. Lou, P.H. Fan, Chemical constituents of hemp (*Cannabis sativa L.*) seed with potential anti-neuroinflammatory activity, Phytochem. Lett. 23

(2018) 57–61, https://doi.org/10.1016/j.phytol.2017.11.013.
[14] W.Q. Chang, Y. Li, M. Zhang, S. Zheng, Y. Li, H.X. Lou, Solasodine-3-β-O-D-glucopyranoside kills *Candida albicans* by disrupting the intracellular vacuole, Food Chem. Toxicol. 106 (2017) 139–146, https://doi.org/10.1016/j.fct.2017.05.045.
[15] C.M. Cao, H. Zhang, R.J. Gallagher, B.N. Timmermann, Withanolide artifacts formed in methanol, J. Nat. Prod. 76 (2013) 2040–2046, https://doi.org/10.1021/np400296s.
[16] T. Yoshida, H. Itoh, S. Matsunaga, R. Tanaka, T. Okuda, Tannins and related polyphenols of euphorbiaceous plants. IX. Hydrolyzable tannins with $_1C^4$ glucose core from *Phyllanthus flexuosus MUELL*, chem.pharm.bull. 40 (1992) 53–60, https://doi.org/10.1248/cpb.40.53.
[17] B.T. Luyen, B.H. Tai, N.P. Thao, K.J. Eun, J.Y. Cha, M.J. Xin, Y.M. Lee, Y.H. Kim, Anti-inflammatory components of *Euphorbia humifusa Willd*, Bioorg. Med. Chem. Lett. 24 (2014) 1895–1900, https://doi.org/10.1016/j.bmcl.2014.03.014.
[18] Y. Tian, L.M. Sun, X.Q. Liu, J.X. Dong, Phenols from *Euphorbia humifusa*, China J. Chin. Mater. Med. 5 (2010) 613–615, https://doi.org/10.4268/cjcmm20100516.
[19] T. Yuan, C. Wan, A. Gonzalez-Sarrias, V. Kandhi, N.B. Cech, N.P. Seeram, Phenolic glycosides from sugar maple (*Acer saccharum*) bark, J. Nat. Prod. 74 (2011) 2472–2476, https://doi.org/10.1021/np200678n.
[20] A. Mansour, R. Celano, T. Mencherini, P. Picerno, A.L. Piccinelli, Y. Foudil-Cherif, D. Csupor, G. Rahili, N. Yahi, S.M. Nabavi, R.P. Aquino, L. Rastrelli, A new cineol derivative, polyphenols and norterpenoids from *Saharan myrtle tea* (*Myrtus nivellei*): isolation, structure determination, quantitative determination and antioxidant activity, Fitoterapia. 119 (2017) 32–39, https://doi.org/10.1016/j.fitote.2017.03.013.
[21] T. Ishikawa, K. Kondo, J. Kitajima, Water-soluble constituents of coriander, Chem. Pharm. Bull. 51 (2003) 32–39, https://doi.org/10.1248/cpb.51.32.
[22] D.X. Sha, Y.H. Liu, L.S. Wang, S.X. Xu, Studies on the chemical constituents of common leafflower(*Phyllanthus urinaria*), J. SPU 17 (2000) 176–178, https://doi.org/10.3969/j.issn.1006-2858.2000.03.007.
[23] S.H. Wu, Y.M. Shen, Y.W. Chen, Z.Y. Li, L.Y. Yang, S.L. Li, Chemical constituents from the stem bark of *Trewia nudiflora*, Chem. Nat. Compd. 45 (2009) 536–538, https://doi.org/10.1007/s10600-009-9386-y.
[24] C.B. Cui, Q.C. Zhao, B. Cai, X.S. Yao, H. Osadsa, Two new and four known polyphenolics obtained as new cell-cycle inhibitors from *Rubus aleaefolius Poir*, J. Asian Nat. Prod. Res. 4 (2002) 243–252, https://doi.org/10.1080/10286020290003692.
[25] E.F. Batista, D.M. Costa, G.M. Guilhon, A.H. Muller, L.S. Santos, M.S. Arruda, A.C. Arruda, M.N. Silva, J.K. Silva, R.S. Secco, A.P. Souza Filho, B.A. Figueira, Chemical constituents and allelopathic and antioxidant activities of *Alchorneopsis floribunda Mull. Arg.* (Euphorbiaceae), Nat. Prod. Res. 27 (2013) 1–8, https://doi.org/10.1080/14786419.2011.643549.
[26] B. Sritularak, N. Boonplod, V. Lipipun, K. Likhitwitayawuid, Chemical constituents of *canarium subulatum* and their anti-herpetic and DPPH free radical scavenging properties, Rec. Nat. Prod. 7 (2013) 129–132.
[27] I.S. Lee, S.H. Jung, J.S. Kim, Polyphenols from *Euphorbia pekinensis* inhibit AGEs formation in vitro and vessel dilation in Larval Zebrafish in vivo, Planta Med. 84 (2018) 176–181, https://doi.org/10.1055/s-0043-120447.
[28] S. Li, S.J. Dai, R.Y. Chen, D.Q. Yu, Triterpenoids from the stems of *Myricaria paniculata*, J. Asian Nat. Prod. Res. 7 (2005) 253–257, https://doi.org/10.1080/10286020410001721168.
[29] W.H. Li, S.T. Chang, S.C. Chang, H.T. Chang, Isolation of antibacterial diterpenoids from Cryptomeria japonica bark, Nat. Prod. Res. 22 (2008) 1085–1093 https://doi.org/10.1080/14786410802267510.
[30] S.H. Yang, H.Z. Guo, D.A. Guo, J.H. Zheng, Studies on chemical constituents of hairy root of *Cassia obtusifolia*, China J. Chin. Mater. Med. 31 (2006) 217–219, https://doi.org/10.3321/j.issn:1001-5302.2006.03.012.
[31] L. Gao, J.P. Wang, H. Tian, P.J. Lu, Y.F. Wang, Chemical constituents of *Sapium sebiferum* leaves, China J. Chin. Mater. Med. 40 (2015) 1519–1522, https://doi.org/10.4268/cjcmm20150818.
[32] M.S. Ali, M.K. Pervez, M. Saleem, R.B. Tareen, Haplophytin-A and B: the alkaloidal constituents of Haplophyllum acutifolium, Phytochemistry. 57 (2001) 1277–1280, https://doi.org/10.1016/S0031-9422(01)00188-1.
[33] F.Q. Wang, J.W. Zhang, G. Zhang, Y.H. Zhang, G.M. Yao, Y.Z. Chen, Y.B. Xue, L.Z. Luo, Chemical constituents of *Sapium sebiferum* leaves, Chin. Pharm. J. 48 (2013) 1908–1911.
[34] O. Dai, L. Yang, Q.M. Zhou, C. Peng, Chemical constituents from tubers of *Bletilla striata*, Chin. J. Exp. Tradit. Med. Formulae. 24 (2018) 43–47.
[35] A. Panthong, D. Kanjanapothi, Y. Thitiponpunt, T. Taesotikul, D. Arbain, Anti-inflammatory activity of the alkaloid bukittinggine from *Sapium baccatum*, Planta Med. 64 (1998) 530–535, https://doi.org/10.1055/s-2006-957508.